

Rhodomonas PE545 fluorescence is increased by glycerol

Chanoknard Karnjanapak^a, I-Shuo Huang^b, Preyanut Jaroensuk^a, Sutaporn Bunyajetpong^{a,*}, Paul V. Zimba^c, F. Gerald Plumley^{a,d}

^a Department of Marine Science, Faculty of Science, Chulalongkorn University, Bangkok 10330 Thailand

^b Virginia Institute of Marine Science, Gloucester Point, Virginia 23062 USA

^c Center for Coastal Studies, Texas A&M University Corpus Christi, Corpus Christi, Texas 78412 USA

^d Aquatic Resources Research Institute, Chulalongkorn University, Bangkok 10330 Thailand

*Corresponding author, e-mail: sutaporn.b@chula.ac.th

Received 5 Dec 2020

Accepted 27 May 2021

ABSTRACT: Phycobilins are photosynthetic pigments found in three ecologically important groups of algae: cyanobacteria, red algae, and cryptophytes. These compounds are covalently attached to proteins, which can be technically difficult to analyze compared with other photosynthetic pigments (e.g., chlorophylls and carotenoids). In this study, glycerol was demonstrated to uncouple PE545 (phycoerythrin 545), the phycobilin complex of *Rhodomonas* spp., from its role as a light-harvesting pigment: the fluorescence signal was increased 15–34 times, and ETR (electron transport rate) was no longer light-dependent at high light intensities. Glycerol induced fluorescence provided a simple and inexpensive protocol to ascertain the pool size of autofluorescent PE545 as well as total PE545 cell content in *Rhodomonas*. 20–30% glycerol was optimal for monitoring increased PE545 fluorescence with a stable signal for at least 1 h after glycerol addition. A substantial portion of PE545 passed through different-sized filter pads in cells with added glycerol, which suggests that glycerol may facilitate extraction of this pigment-protein complex from *R. salina*, a process that can be difficult under certain growth conditions. However, at high concentrations and/or after extended periods of contact, glycerol reduced recovery of PE545, suggesting destruction of the compound. In another approach, we found that PE545 can be recovered from acetone-extracted cells using low concentrations of SDS (sodium dodecyl sulfate) in low pH buffers. The finding provides samples for analyses of both chlorophylls and carotenoids in acetone and PE545 from the cell pellet. *Rhodomonas* spp. plays an important role in nature; hence methods presented here should help determine its natural abundance and distribution.

KEYWORDS: cryptophyte, *Rhodomonas salina*, pigment, phycoerythrin, chlorophyll

INTRODUCTION

Phycobilins play a critical role as photosynthetic light-harvesting antenna in red algae, cyanobacteria, glaucophytes, and cryptophytes. They facilitate utilization of spectral regions that, otherwise, are absorbed poorly by chlorophylls (Chl) and carotenoids. Phycobilin-containing algae and cyanobacteria are important members of the phytoplankton and/or the benthic communities in many freshwater, brackish, and marine habitats. The phycobilin structure is an open-chain tetrapyrrole chromophore covalently attached to apoproteins, collectively termed a phycobiliprotein. The covalent attachment of bilins to proteins conveys a unique biophysical characteristics that alters the biochemistry in such a way that they are challenging to extract and analyze [1, 2]. Phycobilins lack pho-

tochemical activity, but funnel excitation energy to photosynthetic reaction centers (either PSI or PSII). Phycobilin autofluorescence refers to the emission of light energy as fluorescence, rather than the normal/typical transfer of energy to photosynthetic reaction centers [3]. A few species exhibit high phycobilin autofluorescence, indicating that at least some of the pigments are not connected to the photosynthetic apparatus. *In situ* phycobilin autofluorescence was part of the rationale that led to the use of glycerol to completely uncouple phycobilins in *Synechococcus* spp. [3] and the development of a strategy for use of glycerol to identify, quantitatively and qualitatively, the abundance of this ubiquitous and ecologically important cyanobacterial species in natural samples [4]. *Rhodomonas* spp., a cryptophyte, also has high phycobilin autofluorescence from PE545, the red colored antenna pigment (phy-

coerythrin, PE). A preliminary study [5] provides evidence that glycerol increases PE545 fluorescence in *R. salina*. The data presented here support and extend these initial observations.

Methods for analysis of cryptophyte phycobilins, such as the red-colored PE545 light-harvesting complex of *Rhodomonas* spp., are either time-consuming, preparation intensive, or both. It is useful to separate phycobilin methods into two steps, extraction and analysis. The first step, extraction, can be accomplished in some *Rhodomonas* isolates with ease and very high efficiency [2], while extraction in other strains requires elevated temperatures [6] or detergents [1, 5]. Even with complete or nearly complete extraction, the second step, analysis, can be difficult and/or not adequately described in experimental methods. The quantification, an important component of analysis, routinely involves spectrophotometric measurement of absorbance, which can be difficult when samples contain contaminants with overlapping absorption bands (e.g., Chl-protein complexes). Zimba [1] discussed the inherent issues and problems associated with the seemingly simple and time-honored spectrophotometric analysis of phycobilins. In other words, time-intensive steps [7] may be unavoidable, which limits experimental work to only a handful of samples and virtually eliminates field studies, such as ship-board based work. The simple, rapid, and inexpensive means of phycoerythrin analyses in *Synechococcus* spp. using glycerol is a welcome addition to the arsenal for these cyanobacteria [3, 4]. The current study extends this glycerol-based technique to a cryptophyte, *Rhodomonas* spp.

Rhodomonas spp. is arguably the most important and/or most commonly observed cryptophyte in nature, and it also grows well in laboratory cultures. *Rhodomonas* spp. thrives in turbid and low light environments due to its highly efficient green light harvesting phycobiliproteins and unique dual light-harvesting systems; and/or because it relies upon a variety and flexibility of trophic strategies (i.e., photo-, mixo-, hetero-, and phagotrophy) for carbon and energy assimilation. Cryptophytes are considered the preferred or optimal prey for numerous protist and mesozooplankton grazers [8]. The heavy grazing pressure may lead to low cell numbers of cryptophytes in nature, which belies the importance of these algae in the ecosystem food web. Despite heavy grazing pressures, cryptophytes can occur at high densities in nature under certain conditions [9–11].

In this report, we provided details of techniques

that permitted simple and reliable qualitative assessment of phycobiliproteins from a common cryptophyte, *Rhodomonas* spp. The glycerol technique is similar to a technique used with *Synechococcus* spp., an ecologically important cyanobacterium [3, 4], and *Prochlorococcus marinus* [12]. The technique used for *Rhodomonas* spp. in this study relied on glycerol to uncouple phycobiliproteins from transferring excitation energy to the PSI and/or PSII reaction centers, with formation of unique identifiable fluorescence emissions from the phycobilins. The use of glycerol to identify *Synechococcus* spp. in coastal and estuarine habitats has become widespread [13, 14]. Since the seminal work with glycerol-induced fluorescence in *Synechococcus* spp. [3, 4], another cyanobacterium *P. marinus* [12] and now *Rhodomonas* have been shown to share this glycerol-dependent phenotype, making it potentially more difficult to correctly interpret results in ecosystems where these species co-exist. The results and implications of this technique with *Rhodomonas* spp. were also reported in the present study.

MATERIALS AND METHODS

Algal cultures

Two *Rhodomonas* cultures were maintained at either the Chulalongkorn University (CU), Bangkok, Thailand, or the Center for Coastal Studies (CCS), Texas A&M University Corpus Christi, Texas, USA. *Rhodomonas salina*, kindly provided by Saskia Ohse and Dr. Alexandra Kraberg (Alfred Wegener Institute, Helgoland, Germany), was grown at CU in Daigo IMK medium (pH 8) made from commercially available pre-mix packages (Wako Pure Chemical Industries, Ltd., Japan) using filtered seawater (GF/C filter paper, 1.2 μm porosity) at 28 ppt prior to autoclave sterilization. Cultures were maintained at 25 °C under a photon flux of 54 $\mu\text{mol m}^{-2} \text{s}^{-1}$ using cool white fluorescent illumination with light:dark cycles of 12:12 h. The second *Rhodomonas* strain used in this study, Flour Bluff Texas (R-FBT), was isolated from Nueces Bay, Texas and was grown at CCS. Cultures were maintained at 20 °C in f/2 media at 32 ppt under a photon flux of 30 $\mu\text{mol m}^{-2} \text{s}^{-1}$ with light:dark cycles of 12:12 h. For the first strain, small aliquots (~1 ml) of rapidly growing *R. salina* culture were transferred to 250 ml Erlenmeyer flasks containing 125 ml of fresh culture medium; cells in early exponential phase growth (i.e., approximately 2 days after inoculation) were used for analysis. Some data reported here were extracted from an MSc thesis [5]; for these experi-

Table 1 Increases of glycerol-induced fluorescence of PE545 in *R. salina* under different growth regimes and/or with different glycerol concentrations.

Glycerol concentration	Media ^a	Culture age ^b	F585 increase ^c	Reference
20 or 30% glycerol	D-IMK	EE	25–33	This study
20 or 30% glycerol	D-IMK	LS	15–19	This study
20% glycerol	D-IMK	LLS	24–34	This study
50% glycerol	f/2	ES	11	[5]
50% glycerol	D-IMK	ES	22	[5]

^a media used: either Diago IMK (D-IMK) or f/2.

^b culture age: EE = early exponential (approximately 2 days after inoculation), ES = early stationary (8–10 days post inoculation), LS = late stationary (12–14 days post inoculation), LLS = late-late stationary (19–21 days post inoculation).

^c the glycerol-induced signal (F585) strength relative to the autofluorescence signal (F587) in control cells (i.e., F585 was X times larger than F587).

ments, *R. salina* was grown in f/2 medium (Guillard 1975) in larger flasks (i.e., 150–250 ml of rapidly growing *R. salina* was transferred to 1200 ml in 2.5 l flasks) and cells were collected in either early stationary or late stationary phases (i.e., 8–10 or 19 days, after inoculation, respectively). Most data presented in this report for *R. salina* involved cells grown in Diago IMK that were harvested 2 days after inoculation; however, results from other media and/or duration of growth are also reported and are clearly indicated in Table 1.

Steady state fluorescence assays

For glycerol-induced fluorescence, *R. salina* cells were diluted to minimize/prevent re-absorption of fluorescence emissions [15]. Undiluted samples were scanned and preliminary fluorescence emission recorded; samples were diluted and scanned to ensure that signal strength was sufficiently strong for identification of peaks, but not off scale. Cultures with added glycerol were diluted with fresh medium to reach final glycerol concentrations of 0–80% (v/v). Steady-state room temperature fluorescence of *R. salina* was measured following Wyman [4] with some modifications. Fluorescence spectra were recorded on a Perkin Elmer model LS 55 Luminescence Spectrometer (Perkin Elmer Instruments, USA) with both emission and excitation slits of 5 nm and 100 nm/min scan speeds. Samples were scanned 2–6 times, depending on the signal/noise ratios, and a single spectrum was generated for each sample based on a simple arithmetic average at each wavelength. Samples were separately excited with light at 440 nm (Chl *a*), 470 nm, 475 nm (Chl *c*), 490 nm (alloxanthin), or 520 nm (PE545); and emission spectra of the excited samples were recorded at individual wavelengths start-

ing at 10 nm beyond the excitation light and extending to 750 nm. A brief explanation of why we used 520 nm excitation is warranted. The 520 nm light is blue shifted relative to the major absorption band of PE545, but was utilized with high efficiency, and equally important are two additional factors for choosing 520 nm: (1) the fluorescence emissions of PE545, at F585 or F587, was minimized and (2) excessive leakage of the excitation beam into the emission detector was also minimized. Excitation spectra were recorded for specific emission signals; emissions at 685 nm (F685), 705 nm (F705) and 640 nm (F640) were proxies for PSII, PSI and PE545, respectively. The F645 signal is outside the absorption bands of PE545 but is within the range of reported fluorescence emissions for PE545 and is easily distinguished from signals arising from free Chl, LHCs (Light-Harvesting Complexes) and/or PSII.

Steady state fluorescence spectrum, correction and deconvolution

Fluorescence emission spectra were corrected for Photomultiplier Tube (PMT) sensitivity, and excitation spectra were deconvoluted into overlapping Gaussian bands [16]. Briefly, the LS 55 instrument is shipped with a PMT with low sensitivity at long wavelengths; a red-sensitive PMT (e.g., R928, RCA4832) is recommended for analyses of glycerol-treated *Synechococcus* spp. [4] and cryptophytes [7]. Emission spectra were corrected by arithmetic division of *R. salina* spectra by correction factors, which allowed visualization of data as if a R928 red-sensitive PMT had been available. The long wavelength correction factors were generated based on the correction protocols of Perkin Elmer manufacturer. The printed spectra were manually

digitized and used to calculate wavelength-specific correction factors over the range of interest (i.e., 530–750 nm). Excitation spectra of *R. salina* treated with glycerol were deconvoluted into overlapping Gaussian peaks using Excel Solver, an optimization Add-in for Excel; and spectra were not corrected for PMT sensitivity before analysis, as these qualitative results were marginally impacted by PMT sensitivity over the range of analysis (i.e., from ~450 to ~600 nm), as the standard PMT has good sensitivity in this wavelength range.

Pulsed amplitude modulated (PAM) fluorescence assays

Exponential phase cells of *Rhodomonas* sp. (R-FBT) were exposed to 0, 10, 20, 40, or 75% glycerol to determine the efficiency of phycobilisome decoupling by glycerol. Treated cells were incubated at 20 °C for 5 min prior to examination at 525 (± 5) nm excitation and 685 (± 5) nm relaxation using BioTex Synergy HT plate reader (BioTek Instruments, Inc., USA). An additional experiment determined effects of 20% glycerol on *Rhodomonas* sp. (R-FBT). Photosynthetic ability (Chl *a* fluorescence yield) was determined using a WALZ pulse amplitude modulation (PAM), and relaxing fluorescence was determined as previously described [17].

Other procedures

Cell densities were determined using a Neubauer Improved Brightline hemocytometer (0.0025 mm²). Triplicate 1.0 ml aliquots were taken from each culture, and triplicate 10 μ l subsamples were counted from each aliquot.

RESULTS AND DISCUSSION

Fluorescence emission spectroscopy

Growth curves showed that *R. salina* reached the same cell density in *f*/2 as in Daigo IMK, but after a short lag period in *f*/2; PE545 was relatively easy to extract from cells grown in *f*/2 medium, but was recalcitrant to extraction in Daigo IMK [5]. Daigo IMK has 2.6 times higher nitrate and contains ammonia and vitamins. We have not yet determined which of these factors (higher nitrate, addition of ammonia and/or addition of vitamins) is responsible for changes in PE545 extraction. Regardless, the following data are for *R. salina* grown in Daigo IMK (except as noted in Table 1).

The room temperature and steady state fluorescence emission of *R. salina* had low yield (Fig. 1a), as expected for cells in early exponential phase of growth. Excitation energy is transferred with high

efficiency to PSI and/or PSII and used to drive ATP production and/or CO₂ fixation. There were two conspicuous fluorescence emission peaks in the control cells (Fig. 1a): one at 685 nm (F685), previously associated with PSII [18]; and a larger peak at 587 nm (F587), previously associated with a pool of PE545 and not functionally connected to PSI or PSII [19, 20]. This pool of PE545 is also referred to as the autofluorescent pool. There was a third, very small, peak at 702 nm (F702) likely associated with PSI. F702 in *Rhodomonas* spp. has very low signal strength at room temperature [18] which is difficult to detect. A fluorescence signal from Chl *a/c* complexes was not observed, even when the excitation wavelength was at 440 or 465 nm, the peak absorption bands for Chl *a* or *c*, respectively.

The room temperature and steady state fluorescence emission of *R. salina* was increased substantially following addition of glycerol, with the largest emission peak at 585 nm (F585), similar to the autofluorescence peak (F587) described above (Fig. 1b-g and Table 1). The increased fluorescence yield at F585 appeared within seconds after glycerol addition, an observation consistent with the PE-associated signal observed in *Synechococcus* spp. treated with 50% glycerol [4]. The increased fluorescence signal was relatively stable for at least 1 h after glycerol addition (Fig. 1c-f), though the large increases were somewhat reduced in intensities with longer exposure times (i.e., longer than 1 h, data not shown). Addition of glycerol had minimal effects on the pH of the growth medium, with only a small increase/decrease of signal. The effects of glycerol addition on the steady-state fluorescence yield of *R. salina* were verified in at least 12 independent experiments and are summarized in Table 1.

Glycerol concentrations of 20 to 30% routinely and reproducibly resulted in the greatest increase of F585 signal in *R. salina* (Fig. 1cd) at 15–34 times compared with untreated cells depending upon culture conditions (e.g., media used and/or age of culture post inoculation; Table 1). F585 was also increased in 40 and 50% glycerol (Fig. 1ef) but less so than at 20–30% glycerol. At very high glycerol concentrations (i.e., 80%), F585 was of low intensity and shifted 5–7 nm toward the blue (to F579, Fig. 1g); similar shifts were observed previously in purified PE545 and ascribed to denaturation of pigments and/or disruption of pigment-pigment and/or pigment-protein interactions within PE545 [5, 7]. At optimal concentrations of glycerol (i.e., 20 or 30%), F585 was stable for at least 1 h following addition of glycerol (Fig. 1cd).

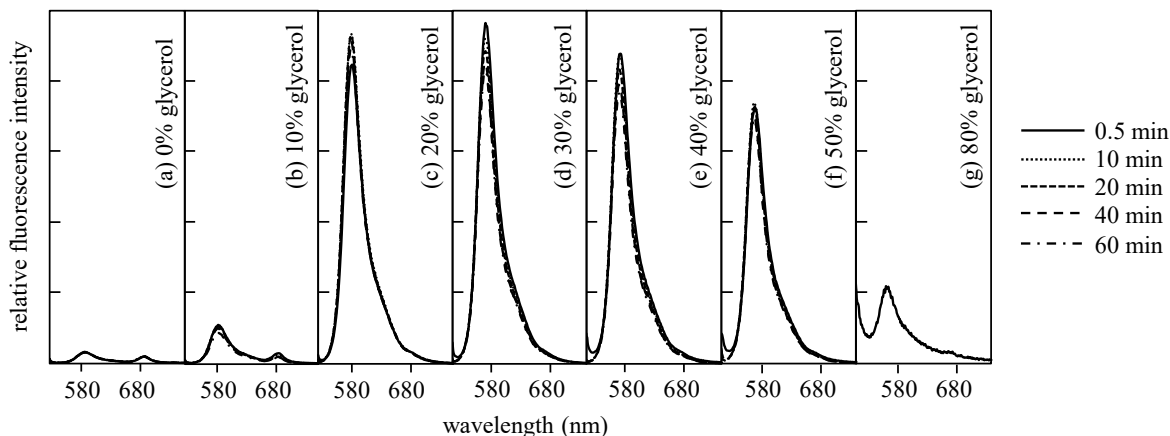


Fig. 1 *In vivo* steady state fluorescence emissions arising from 520 nm excitation of *R. salina* treated with different concentrations of glycerol (0–80%, a–g) at various periods of time (0.5–60 min). A time-series for the 80% glycerol sample was not conducted, as the signal was initially low and did not change appreciably over 1 h.

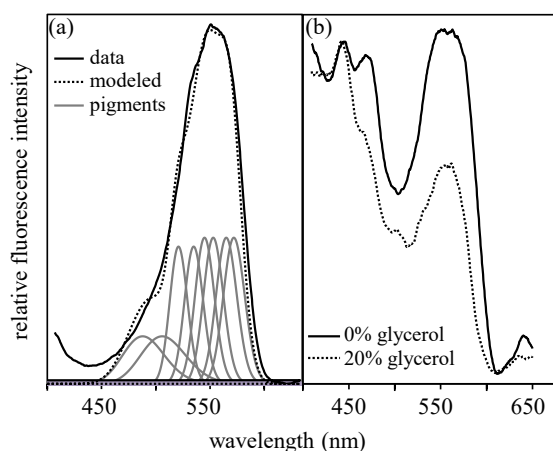


Fig. 2 *In vivo* excitation spectra of *R. salina*. In (a), the data for cells in 20% glycerol with fluorescence emission at 645 nm were plotted with the modeled data derived by curve deconvolution based on the eight known pigments of PE545 at the absorption maxima of 488, 506, 521, 535, 545, 553, 565, and 572 nm, respectively. In (b), the two spectra for cells in either 0% or 20% glycerol with fluorescence emission at 685 nm were normalized to their respective Chl *a* excitation maxima at ~440 nm.

Fluorescence excitation spectroscopy

The fluorescence emission of glycerol-treated *R. salina* peaked at F585, but the spectrum had a very broad line shape, extending well beyond F585 into longer wavelengths (Fig. 1c–f). These red emission signals could arise from Chl-protein complexes (e.g., PSI, PSII, or Chl *a/c*) or from

PE545, which is known to have a ‘red tail’ of fluorescence. To distinguish these possible origins of the fluorescence emission in glycerol-treated cells, excitation spectra were generated for a number of wavelengths (i.e., every 5 nm from 585–710 nm). The F645 signal was chosen for detailed presentation (Fig. 2a) because this wavelength was considerably longer than the primary F585 peak but was near a long wavelength fluorescence shoulder of PE545 [20] associated with two MBV pigments on the α_1 and α_2 subunits [18]. Moreover, it was considerably blue shifted relative to emission peaks expected for Chl *a/c* (683 nm), PSII (685 nm), or PSI (702 nm). In other words, the F645 signal was easily ascribed to PE545, and it could be readily distinguished from Chl-protein signals.

The *in vivo* excitation spectrum of F645 in cells treated with 20% glycerol had a major peak at 545 nm with a shoulder at 568 nm (Fig. 2a). The shape of the excitation spectrum was similar to the absorption spectrum of isolated PE545 [5, 20] and was well modeled by eight bands, one for each of the eight pigments in the PE545 heterodimer (Fig. 2a). The two excitation bands on the blue edge (i.e., 488 and 506 nm) had less intense signals and broadened absorption features in glycerol-treated cells, similar to those in isolated PE545 [20]. However, the presence of an absorption band at 488 nm is not expected for PEB absorption, but it has been reported previously in *R. salina* [21].

The following data were generated to answer a straight-forward question: was the increase of fluorescence induced by glycerol (Fig. 1) related solely

to PE545, or did Chl-protein complexes contribute to the signal? In brief, the excitation spectrum for F645 (Fig. 2a) provided evidence that the fluorescence ‘red tail’ was derived from PE545 but did not rule out contributions from Chl-protein complexes, especially at wavelengths longer than 645 nm. It is important to point out that it would not be surprising to have F signals from Chl-protein complexes in these spectra, as they were generated using ‘whole cells’ with a full complement of Chl *a/c*, PSII, and PSI; and no steps had been taken to separate these Chl-protein complexes before fluorescence assays were performed. For instance, PE545 could be physically and energetically coupled to Chl *a/c* and/or PSII after glycerol treatment; and this would give an excitation spectrum with a large PE545 component, though the emission would be from one (or both) of the Chl-protein complexes with high fluorescence when uncoupled from the electron transport chain. To determine the extent, if any, that Chl *a/c* and/or PSII contributed to the fluorescence ‘red tail’, excitation spectra for F685 nm in glycerol-treated *R. salina* was examined and compared to the excitation spectra for F685 in cells without glycerol (Fig. 2b). In the control cells (without glycerol), F685 excitation energy was derived from pigments with absorption bands corresponding to Chl *a* (440 nm), Chl *c* (465 nm), and PE545 (545 nm peak with a shoulder). The same absorption bands, with peaks at 440, 465, and 545 nm, were present in glycerol-treated cells; but the relative strengths of these signals were very different from those in the control cells. The contributions from both Chl *c* and PE545 were greatly reduced compared with the contribution from Chl *a* following addition of glycerol (Fig. 2b). The most straightforward explanation for these results was that F685 excitation comes from three potential sources in the control cells: (1) the two core antenna CP685 and CP695 of PSII, (2) Chl *a/c* complexes, and (3) PE545; all three of which were energetically coupled in the control cells. In contrast, F685 excitation in glycerol-treated cells arose from only two sources, a relatively small F signal from the core antenna of PSII (i.e., CP685 and CP695) and a larger F signal from the ‘red tail’ of PE545, a light-harvesting complex that was no longer energetically coupled to PSII. Stated differently, PE545 was energetically coupled to PSII in the control cells resulting in fluorescence emission at 685 nm, while PE545 in the glycerol-treated cells was no longer coupled to PSII and, as a result, gave rise to a F585 signal that extended to, and overlapped with, PSII at F685.

The excitation spectrum of F702 (data not shown), associated with PSI in the control cells, was qualitatively similar to the excitation spectrum of F685 (Fig. 2b); but the extremely low fluorescence yield of PSI in *R. salina* and the low sensitivity of the PMT used in this study at 702 nm made it difficult to draw definitive conclusions, as the signal/noise ratio in the 400–450 nm range complicated the data analysis. Despite these limitations, the F702 excitation spectrum in cells treated with 20% glycerol appeared to be similar to the excitation spectrum of F685, with a major contribution from Chl *a* and a larger signal associated with the ‘red tail’ of uncoupled PE545 (data not shown).

The fluorescence excitation spectroscopy data in Fig. 2 provided strong evidence that the glycerol-mediated increase in the fluorescence signal of *R. salina* was overwhelmingly from pigments whose absorption properties mirrored those of PE545 when fluorescence was excited at 520 nm and emission measured at 585 nm (Fig. 2a; and other wavelengths in the 550–600 nm range, data not shown). Moreover, these data provided evidence, but not a proof, that the long ‘red tail’ of fluorescence observed in glycerol-treated *R. salina* arose from PE545. Although a ‘red tail’ fluorescence emission signal can be seen in spectra of isolated PE545, it was not clear if this signal would be preserved in the presence of glycerol; and the following work addressed this issue.

Fluorescence analysis of supernatants and filtrates of *R. salina* treated with glycerol

The effect of glycerol, if any, on the ‘red tail’ of PE545 was investigated with three complementary approaches. In the first approach, we used light microscopy and epifluorescence microscopy of glycerol-treated *R. salina* to show that glycerol addition resulted in cell rupture and release of intracellular constituents into the growth medium; while the extracellular pool contained very small particles with fluorescence properties qualitatively similar to those of the control cells (i.e., cells not treated with glycerol). The glycerol induced rupture of *R. salina* was not expected; we expected to see cells shrink. We explained this rupture based on glycerol acting as tonicity [22].

In the second approach, it was hypothesized that a portion of the PE545 pool had been released into the extracellular pool and that the F585 signal would remain in suspension following low speed centrifugation ($13\,000 \times g$ for 5 min) of the glycerol-treated cells, which should sediment whole cells,

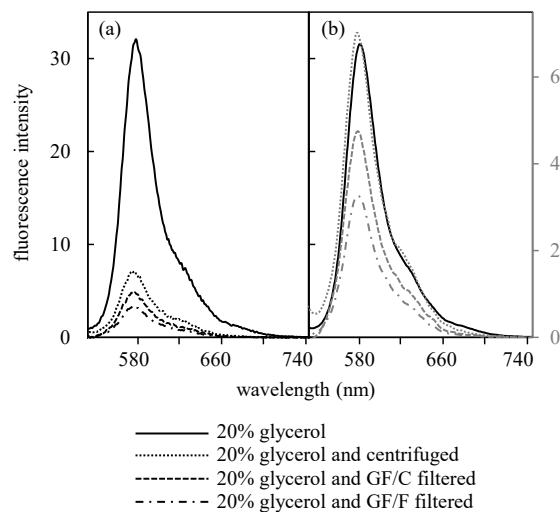


Fig. 3 Steady state fluorescence emissions arising from 520 nm excitation of *R. salina*. Cells treated with 20% glycerol (control) were either centrifuged at $13\,000 \times g$ for 5 min before analysis of the supernatant or filtered through either GF/C or GF/F before analysis of the filtrates. The four emission spectra in (a) were plotted on the same scale (left axis) as recorded; in (b), spectra for the control and the centrifugation supernatant were adjusted to the same peak heights and the filtrates plotted on the same scale (right axis) as the supernatant.

but not pigment-protein complexes; and this hypothesis was proved accurate (Fig. 3). The F585 signal in the supernatant of glycerol-treated cells was reduced in intensity following centrifugation by about 70–80%, indicating that about 20–30% of the pigments responsible for F585/87 remained in the supernatant. Qualitatively, the spectral properties of the supernatants of glycerol-treated cells were largely unchanged following centrifugation, especially as related to the F585/87 signals (Fig. 3ab); and signals associated with PSII and/or PSI were still detectable in the supernatant, but with greatly diminished intensity suggesting that they were mostly localized intracellularly (data not shown).

The third approach was based on the observation that a portion of the F585 signal remained in the supernatant following low-speed centrifugation (Fig. 3), therefore it is possible that F585 pigments also passed through filter pads. As a background, a dissolved material in seawater is generally defined as matter that passes through a given filter (e.g., 0.22 or 0.45 μm pore size), whereas a particulate material is retained on the filter pad. Glycerol-

treated cells were subjected to filtration using three different filter pads, with pore sizes of 0.22, 0.45, or 0.7 μm . Results indicated that approximately 4–16% of F585 passed through the filter pads in a pore-size-dependent fashion (Fig. 3a). Looking at the material that passed through the GF/C and GF/F filters in more details, the emission peaks were centered at 585 nm, identical to F585 signals before filtration; and the filtrate emission spectra also exhibited pronounced ‘red tail’ that extended to 750 nm (Fig. 3ab). The excitation spectra of the two filtrates were devoid of Chl *a* and Chl *c* contributions (i.e., absorption at 440 nm and 465 nm, respectively; data not shown).

PAM analysis of *Rhodomonas* sp. treated with glycerol

The effects of glycerol were assessed on the second strain of *Rhodomonas* (R-FBT) using Pulse Amplitude Modulated (PAM) fluorescence. PAM fluorescence provides a non-invasive means of measuring photosynthetic electron flow (ETR), particularly the electron flow around PSII reaction center [23]. Initial experiments showed that 10% glycerol minimally impacted ETR and yield, while glycerol concentrations of 20% or greater had dramatic effects that were independent of glycerol concentrations (data not shown). Data for 20% glycerol are detailed with both ETR (Fig. 4a) and yield (Fig. 4b) followed the expected light response curves, with increased ETR and reduced yield as light intensity (PAR) increased. In contrast, ETR was reduced to levels that were near instrument detection limits in glycerol-treated cells (Fig. 4a) but did appear to exhibit PAR dependent increases at the lower light intensities tested (Fig. 4a). For the ETR values of regular cells which kept rising in the control sample (Fig. 4a), it can occur and be related to microalgal strain, cultivation conditions, physiological status, and microalgal growth [24]. Yield estimates with glycerol-treated cells are informative but likely unreliable because of the low ETR values recorded under this condition (Fig. 4b). Overall, the PAM data clearly indicates in the second strain of *Rhodomonas* (R-FBT) that 20% glycerol had substantial impacts on photochemistry. Similar results were obtained in preliminary experiments with *R. salina* using an AquaPen-C device (data not shown). The PAM data, combined with photomicrographs (data not shown) and filtration data (Fig. 3), strengthen the hypothesis that glycerol effects extended beyond uncoupling PE545 from its role as a light-harvesting pigment and extended to other photochemical processes.

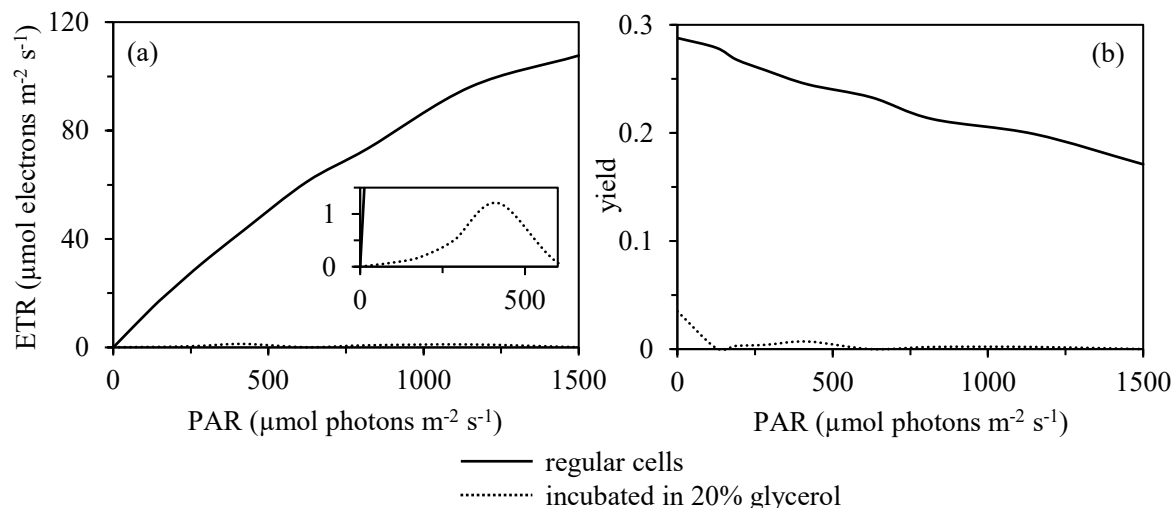


Fig. 4 ETR (a) and yield (b) of the control and the 20% glycerol-treated *Rhodomonas* (R-FBT strain) measured with PAM.

Non-photochemical Quenching (NPQ, Fig. S1) measured in *R. salina* with and without addition of 20% glycerol also supported the PAM data.

CONCLUSION

Rhodomonas spp. is an abundant and important prey source ecologically. This study describes a simple procedure, based on glycerol-induced increases in fluorescence emission of PE545, for rapid analyses of phycobilins in *Rhodomonas* spp. 20–30% glycerol was optimal for short-term experiments, while higher concentrations or prolonged exposure to glycerol could be deleterious to PE545 stability. For field work, results shown here with *Rhodomonas* spp. strongly suggest that size-fractionated filtration should be included as part of the procedure to allow clear separation of large cells, such as *Rhodomonas* spp., from small cells, such as *Synechococcus* spp., while simultaneously eliminating other cells that potentially could confound interpretation of results. The inclusion of size fractionation would seem especially important in coastal waters and/or waters collected near the bottom of the euphotic zone, areas likely to have abundant cryptophytes. One potentially fertile area for future research lies in evaluation of increases in fluorescence induced by glycerol with other pigmented cryptophytes. In other words, is *Rhodomonas* spp. unique, or do other cryptophytes share this trait?

Appendix A. Supplementary data

Supplementary data associated with this article can be found at <http://dx.doi.org/10.2306/scienceasia1513-1874.2021.062>.

Acknowledgements: The study was financially supported by the 90th Anniversary of Chulalongkorn University Scholarship, Grants for Development of New Faculty Staff (Ratchadaphiseksomphot Endowment Fund) and Visiting Professorship (Kanchanaphisek Chalermphrakiat Endowment Fund). Our sincere thanks are given to Assoc. Prof. Dr. Thaithaworn Lirdwitayaprasit and Ingon Thongcomdee (Algal Culture Laboratory, Department of Marine Science, CU) who provided help with algal cultures.

REFERENCES

1. Zimba PV (2012) An improved phycobilin extraction method. *Harmful Algae* **17**, 35–39.
2. Lawrenz E, Fedewa EJ, Richardson TL (2011) Extraction protocols for the quantification of phycobilins in aqueous phytoplankton extracts. *J Appl Phycol* **23**, 865–871.
3. Wyman M, Gregory R, Carr N (1985) Novel role for phycoerythrin in a marine cyanobacterium, *Synechococcus* strain DC2. *Science* **230**, 818–820.
4. Wyman M (1992) An *in vivo* method for the estimation of phycoerythrin concentrations in marine cyanobacteria (*Synechococcus* spp.). *Limnol Oceanogr* **37**, 1300–1306.
5. Karnjanapak C (2016) Evaluation of phycobilins in marine cryptomonad *Rhodomonas salina* and marine cyanobacteria *Synechococcus* spp. *Master thesis*, Chulalongkorn Univ, Bangkok, Thailand.

6. Chaloub RM, Motta NMS, de Araujo SP, de Aguiar PF, da Silva AF (2015) Combined effects of irradiance, temperature and nitrate concentration on phycoerythrin content in the microalga *Rhodomonas* sp. (Cryptophyceae). *Algal Res* **8**, 89–94.
7. MacColl R, Malak H, Gryczynski I, Eisele LE, Mizejewski GJ, Franklin E, Hesham S, Montellese D, et al (1998) Phycoerythrin 545: monomers, energy migration, bilin topography, and monomer/dimer equilibrium. *Biochemistry* **37**, 417–423.
8. Johnson MD, Beaudoin DJ, Frada MJ, Brownlee EF, Stoecker DK (2018) High grazing rates on cryptophyte algae in Chesapeake Bay. *Front Mar Sci* **5**, 1–13.
9. Gieskes WWC, Kraay GW (1983) Dominance of cryptophyceae during the phytoplankton spring bloom in the central North Sea detected by HPLC analysis of pigments. *Mar Biol* **75**, 179–185.
10. Wollschläger J, Wiltshire KH, Petersen W, Metfies K (2015) Analysis of phytoplankton distribution and community structure in the German Bight with respect to the different size classes. *J Sea Res* **99**, 83–96.
11. Dubelaar GBJ, Geerders PJF, Jonker RR (2004) High frequency monitoring reveals phytoplankton dynamics. *J Environ Monit* **6**, 946–952.
12. Lokstein H, Steglich C, Hess WR (1999) Light-harvesting antenna function of phycoerythrin in *Prochlorococcus marinus*. *Biochim Biophys Acta* **1410**, 97–98.
13. Williams WP, Saito K, Furtado D (1981) Use of lateral phase separations as a probe of photosynthetic membrane organization. In: Akoyunoglou G (ed) *Photosynthesis III. Structure and Molecular Organisation of the Photosynthetic Apparatus*, Balapan International Science Services, Philadelphia, pp 97–106.
14. Heathcote P, Wyman M, Carr NG, Beddard GS (1992) Partial uncoupling of energy transfer from phycoerythrin in the marine cyanobacterium *Synechococcus* sp. WH7803. *Biochim Biophys Acta Bioenerg* **1099**, 267–270.
15. Mohanty P, Braun BZ, Govindjee (1972) Fluorescence and delayed light emission in Tris-washed chloroplasts. *FEBS Lett* **20**, 273–276.
16. Garlaschi FM, Zucchelli G, Giavazzi P, Jennings RC (1994) Gaussian band analysis of absorption, fluorescence and photobleaching difference spectra of D1/D2/cyt *b*-559 complex. *Photosynth Res* **41**, 465–473.
17. Schreiber U (2004) Pulse-amplitude-modulation (PAM) fluorometry and saturation pulse method: an overview. In: Papageorgiou GC, Govindjee (eds) *Chlorophyll a Fluorescence, A Signature of Photosynthesis*, Springer, The Netherlands, pp 279–319.
18. Doust AB, Wilk KE, Curmi PMG, Scholes GD (2006) The photophysics of cryptophyte light-harvesting. *J Photochem Photobiol A* **184**, 1–17.
19. van der Weij-De Wit CD, Doust AB, van Stokkum IHM, Dekker JP, Wilk KE, Curmi PMG, Scholes GD, van Grondelle R (2006) How energy funnels from the phycoerythrin antenna complex to photosystem I and photosystem II in cryptophyte *Rhodomonas* CS24 cells. *J Phys Chem B* **110**, 25066–25073.
20. Doust AB, Marai CN, Harrop SJ, Wilk KE, Curmi PM, Scholes GD (2004) Developing a structure-function model for the cryptophyte phycoerythrin 545 using ultrahigh resolution crystallography and ultrafast laser spectroscopy. *J Mol Biol* **344**, 135–153.
21. Kana R, Prašil O, Mullineaux CW (2009) Immobility of phycobilins in the thylakoid lumen of a cryptophyte suggests that protein diffusion in the lumen is very restricted. *FEBS Lett* **583**, 670–674.
22. Silverthorn DU (2011) Osmolarity and tonicity: an inquiry laboratory using plant material. In: *Tested Studies for Laboratory Teaching*, Proceedings of the Association for Biology Laboratory Education, **32**, pp 135–150.
23. Schreiber U, Schliwa U, Bilger W (1986) Continuous recording of photochemical and non-photochemical chlorophyll fluorescence quenching with a new type of modulation fluorometer. *Photosynth Res* **10**, 51–62.
24. Malapascua JRF, Jerez CG, Sergejevová M, Figueroa FL, Masojídek J (2014) Photosynthesis monitoring to optimize growth of microalgal mass cultures: application of chlorophyll fluorescence techniques. *Aquat Biol* **22**, 123–140.

Appendix A. Supplementary data

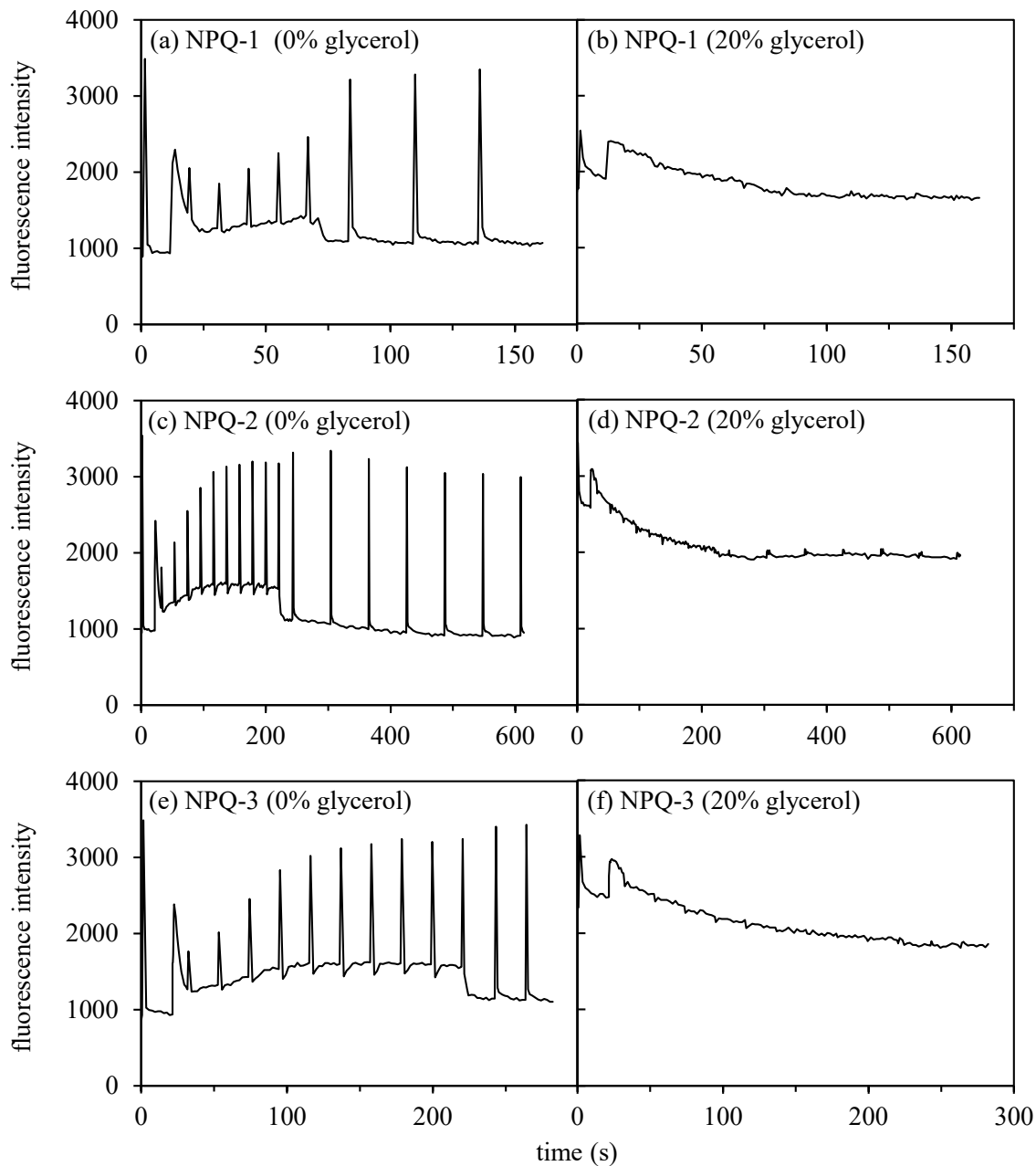


Fig. S1 Non-photochemical quenching (NPQ) of the controls (a, c and e) and the 20% glycerol-treated *R. salina* at day-2 culture (b, d and f), induced during illumination with 450-nm light and measured with AquaPen-C under three predefined profiles (NPQ-1, NPQ-2 and NPQ-3).